INFECTION AND IMMUNITY, May 2003, p. 2724–2735 Vol. 71, No. 5
0019-9567/03/$08.00+0 DOI: 10.1128/IAI.71.5.2724–2735.2003

Rapid Apoptosis Induced by Shiga Toxin in HeLa Cells

Jun Fujii,[1]* Takashi Matsui,[2] Daniel P. Heatherly,[1] Kailo H. Schlegel,[1] Peter I. Lobo,[1] Takashi Yutsudo,[3] Georgianne M. Ciraolo,[4] Randal E. Morris,[4] and Tom Obrig[1]

Department of Internal Medicine/Nephrology, University of Virginia, Charlottesville, Virginia 22908[1]; Faculty of Pharmacy and Pharmaceutical Science, Fukuyama University, Fukuyama City 729-0292,[2] and Discovery Research Laboratory, Shionogi & Co., Ltd., Settsu City, Osaka 566-0022,[3] Japan; and Department of Cell Biology, Neurobiology, and Anatomy, University of Cincinnati Medical Center, Cincinnati, Ohio 45267-0521[4]

Received 17 September 2002/Returned for modification 25 November 2002/Accepted 8 January 2003

Apoptosis was induced rapidly in HeLa cells after exposure to bacterial Shiga toxin (Stx1 and Stx2; 10 ng/ml). Approximately 60% of HeLa cells became apoptotic within 4 h as detected by DNA fragmentation, terminal deoxynucleotidyltransferase-mediated dUTP-biotin nick end labeling (TUNEL) assay, and electron microscopy. Stx1-induced apoptosis required enzymatic activity of the Stx1A subunit, and apoptosis was not induced by the Stx2B subunit alone or by the anti-globotriaosylceramide antibody. This activity was also inhibited by brefeldin A, indicating the need for toxin processing through the Golgi apparatus. The intracellular pathway leading to apoptosis was further defined. Exposure of HeLa cells to Stx1 activated caspases 3, 6, 8, and 9, as measured both by an enzymatic assay with synthetic substrates and by detection of proteolytically activated forms of these caspases by Western immunoblotting. Preincubation of HeLa cells with substrate inhibitors of caspases 3, 6, and 8 protected the cells against Stx1-dependent apoptosis. These results led to a more detailed examination of the mitochondrial pathway of apoptosis. Apoptosis induced by Stx1 was accompanied by damage to mitochondrial membranes, measured as a reduced mitochondrial membrane potential, and increased release of cytochrome *c* from mitochondria at 3 to 4 h. Bid, an endogenous protein known to permeabilize mitochondrial membranes, was activated in a Stx1-dependent manner. Caspase-8 is known to activate Bid, and a specific inhibitor of caspase-8 prevented the mitochondrial damage. Although these data suggested that caspase-8-mediated cleavage of Bid with release of cytochrome *c* from mitochondria and activation of caspase-9 were responsible for the apoptosis, preincubation of HeLa cells with a specific inhibitor of caspase-9 did not protect against apoptosis. These results were explained by the discovery of a simultaneous Stx1-dependent increase in endogenous XIAP, a direct inhibitor of caspase-9. We conclude that the primary pathway of Stx1-induced apoptosis and DNA fragmentation in HeLa cells is unique and includes caspases 8, 6, and 3 but is independent of events in the mitochondrial pathway.

Shiga toxin (Stx)-induced apoptosis is an important process in the pathophysiological response of humans to this bacterial toxin. Apoptosis has been reported in several different cell types as a result of Stx1 and Stx2 action associated with enterohemorrhagic *Escherichia coli* disease, the phases of hemorrhagic diarrhea (38, 46), hemolytic-uremic syndrome (22, 23, 24), and neurological damage (16, 54, 58). All members of the Stx family of toxins (Stxs) are composed of 1A and 5B subunit proteins (43). The A subunit is an *N*-glycosidase that removes adenine 4342 of 28S RNA of the 60S ribosomal subunit (12), rendering ribosomes inactive for protein synthesis (44). Each B subunit (StxB) binds with high affinity to the glycosphingolipid globotriaosylceramide, Gb3 (CD77) (33), present on select eukaryotic cells (32). CD77 antigen is also a marker for B-cell Burkitt's lymphoma (42, 56). Following receptor binding, Stxs are internalized by receptor-mediated endocytosis (49) and are transported directly from early/recycling endosomes to a Golgi apparatus in HeLa cells (13, 35). Brefeldin A is an antiviral substance produced by fungi that inhibits the Golgi apparatus (45) and the processing of Stxs required for inhibition of protein synthesis in HeLa cells (11). The relative importance of Stx-induced apoptosis in human disease is becoming apparent. Indeed, the Stxs cause apoptosis in human renal proximal tubular epithelial cells (29), renal tubular cells (21, 25), human renal cortical epithelial cells (25, 28), lung epithelial cells (55), human endothelial cells (26), astrocytoma cells (4), and Vero cells (19). But the mechanisms of apoptosis have not been fully elucidated. Only in Burkitt's lymphoma cells were extracellular recombinant StxB (36) and an anti-CD77 monoclonal antibody (50) sufficient to induce apoptosis.

Caspase activation is important in the process of apoptosis. Caspases are present as inactive proenzymes, most of which are activated by proteolytic cleavage at specific aspartic amino acid sites (3). Caspase-8, caspase-9, and caspase-3 are situated at pivotal junctions in apoptotic pathways. Caspase-8 is activated in response to extracellular apoptosis-inducing ligands such as tumor necrosis factor alpha (TNF-α) or Fas ligand in a complex of the receptors and cytoplasmic death domains (5). Caspase-9 activates disassembly in response to agents or insults that trigger release of cytochrome *c* from the mitochondria (15, 34) and is activated when complexed with dATP, apoptotic protease activating factor (Apaf-1), and extramitochondrial cytochrome *c* (31).

Several examples of Stx- or Stx2-induced apoptosis have been reported. In the human monocytic cell line THP-1,

* Corresponding author. Mailing address: Department of Internal Medicine/Nephrology, Box 800133, University of Virginia, Charlottesville, VA 22908. Phone: (434) 243-6543. Fax: (434) 924-5848. E-mail: jf4p@hscmail.mcc.virginia.edu.

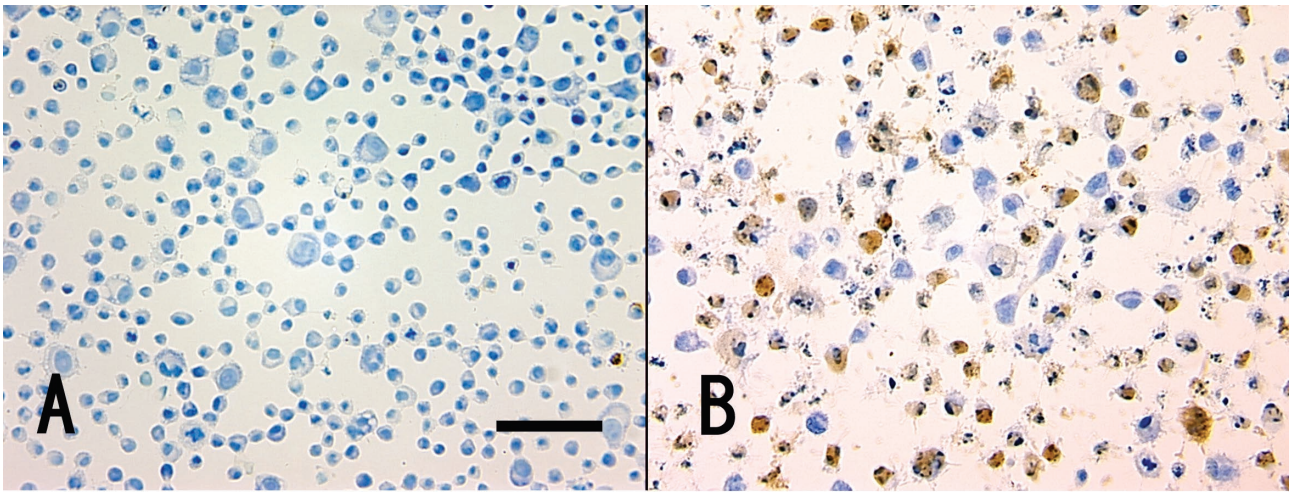

FIG. 1. Apoptotic in situ DNA fragmentation analysis. Cytospin was carried out to attach the apoptotic cells to the glass slide, and apoptosis was monitored by the TUNEL assay. The percentage of TUNEL-positive cells (brown) was 0.60% ± 0.15% in the control (in the absence of Stx1) (A) and 63.7% ± 2.7% after exposure of the cells to Stx1 (10 ng/ml) for 4 h (B).

caspase-3 activation, DNA fragmentation, and chromatin condensation caused by Stxs were blocked by pretreatment with brefeldin A (30). After treatment of THP-1 cells with purified Stx1 or Stx2, caspase-2, -3, -6, -8, -9, and -10-like proteolytic activities increased in the cytosol (30). Specific inhibition of select caspases prevented Stx-induced apoptosis in some cell types such as human endothelial cells. Nakagawa et al. (41) reported that HeLa/C4 cells transfected with the Stx1B subunit induced apoptosis by activating caspase-1 and caspase-3, but the Stx1A subunit gene induced necrosis. Stx1- and Stx2-mediated apoptosis of Hep-2 cells was associated with enhanced expression of Bax (20), known to induce cytochrome *c* release to promote apoptosis (14). The Bcl-2/Bax family is located on the mitochondrial outer membrane, where Bcl-2 blocks Bax-induced cytochrome *c* release from mitochondria (57), preventing apoptosis.

In the present study, we set out to describe a complete pathway of Stx1-induced apoptosis in one cell type, HeLa cells, to serve as a model for comparison of Stx-induced apoptosis in other cell types. The resulting data indicate that a unique apoptotic pathway exists in HeLa cells in response to Stx1. The apoptotic response was rapid, was independent of death domain signaling, involved caspases 3, 6, and 8, and required intracellular processing of Stx1. Interestingly, changes in mitochondrial properties were observed, all of which appeared to be secondary to the apoptotic response.

MATERIALS AND METHODS

Purification of Stx1 and Stx2. Stx1, Stx2, and Stx1B used in this study were purified to homogeneity as described previously (59) and were determined to be free of detectable lipopolysaccharide by the toxicolor test and by sodium dodecyl sufate-polyacrylamide gel electrophoresis and silver staining. The cytotoxic potencies of Stx1 and Stx2 were 10^5 and 10^6 50% cytotoxic doses (CD_{50})/μg of protein, respectively, for 24 h as tested in Vero cells using the WST-1 cell proliferation assay (Wako Chemicals USA, Inc., Richmond, Va.).

Reagents. General caspase inhibitor (Z-Val-Ala-Asp-fmk [Z-VAD-fmk]), caspase-1 inhibitor (Z-Tyr-Val-Ala-Asp-fmk [Z-YVAD-fmk]), caspase-2 inhibitor (Z-Val-Asp-Val-Ala-Asp-fmk [Z-VDVAD-fmk]), caspase-3 inhibitor (Z-Asp-Glu-Val-Asp-fmk [Z-DEVD-fmk]), caspase-6 inhibitor (Z-Val-Glu-Ile-Asp-fmk [Z-VEID-fmk]), caspase-8 inhibitor (Z-Ile-Glu-Thr-Asp-fmk [Z-IETD-fmk]), and caspase-9 inhibitor (Z-Leu-Glu-His-Asp-fmk [Z-LEHD-fmk]) were purchased from Enzyme System Products (Livermore, Calif.). Fluorogenic substrates for caspase-3 (7-amino-4-trifluoromethyl coumarin [AFC]), caspase-6, caspase-8, and caspase-9 were obtained from BIOMOL Research Laboratory Inc. (Plymouth Meeting, Pa.). A rabbit anti-human cytochrome *c* antibody and a purified cytochrome *c* of horse origin were purchased from Research Diagnostics, Inc. (Flanders, N.J.). A horseradish peroxidase-conjugated antibody was obtained from Amersham Life Science (Chicago, Ill.). A fluorescein phycoerythrin (PE)-conjugated mouse monoclonal antibody to human Fas (clone UB2) was obtained from MBL (Nagoya, Japan). Antibodies against human caspase-3, caspase-8, caspase-6, and caspase-9, lamin A, and XIAP were obtained from Cell Signaling Technology (Beverly, Mass.). A human anti-Bid antibody was purchased from Santa Cruz Biotechnology, Inc. (Santa Cruz, Calif.). Brefeldin A and an anti β-actin antibody were purchased from Sigma (St. Louis, Mo.). Hybridoma CRL1907 was purchased from the American Type Culture Collection (ATCC; Manassas, Va.); the monoclonal antibody from the hybridoma reacts with the A subunit of Stx2 and does not react with the B subunit. The Stx2A subunit mutant (Stx2 E166D) was a gift from C. Thorpe. A rat anti-human CD77 monoclonal immunoglobulin M (IgM) antibody (CD77 MAb) was purchased from Coulter (Miami, Fla.).

5,5′,6,6′-Tetrachloro-1,1′,3,3′-tetraethylbenzimidazolcarbocyanine iodide (JC-1) was obtained from Molecular Probes (Eugene, Oreg.).

Cell culture. HeLa cells were grown in RPMI 1640 medium (GIBCO BRL, Grand Island, N.Y.) with 10% heat inactivated (56°C, 30 min) fetal calf serum (FCS; GIBCO BRL) in a 5% CO_2 incubator at 37°C. It is noteworthy that the HeLa cells in this study expressed significantly more Gb3 than the HeLa cells from the ATCC (data not shown). The effects of the Stx1 B subunit, CD77 MAb, and Stx2 E166D on HeLa cells were measured. HeLa cells were plated on 6-well cluster plates (Corning, Inc., Corning, N.Y.) at a concentration of 1.0×10^6 cells in 2 ml of RPMI 1640 with 10% FCS per well and with either Stx1, Stx2 (10 ng/ml), Stx1B (78.5 ng/ml, 785 ng/ml, or 3.96 μg/ml), CD77 MAb (0.5 or 5 μg/ml), or Stx2 E166D (40 ng/ml, 400 ng/ml, or 4 μg/ml). After a 4-h incubation, DNA was extracted using a DNA extraction kit (Sepa Gene; Sankou-Jyunyaku Co. Ltd., Tokyo, Japan).

Standard fixation for transmission electron microscopy. The HeLa cells (10^6) grown in 6-well culture plates were treated with Stx2 (10 ng/ml) for 0 or 4 h. Samples were prepared for transmission electron microscopy as described previously (40). After fixation, infiltration, embedding, and hardening, ultrathin sections were cut with an Ultracut E ultramicrotome using a diamond knife (Diatome, U.S., Fort Washington, Pa.). The sections were picked up onto 300-mesh grids and stained with 2% uranyl acetate and Reynold's lead citrate. Stained grids were viewed with a JEOL 1230 electron microscope operating at 80 kV.

Postembedding immunogold electron microscopy. In those instances where immunogold labeling was used, cells were fixed in an aldehyde fixative that contained a reduced level of glutaraldehyde (Hanks balanced salt solution–

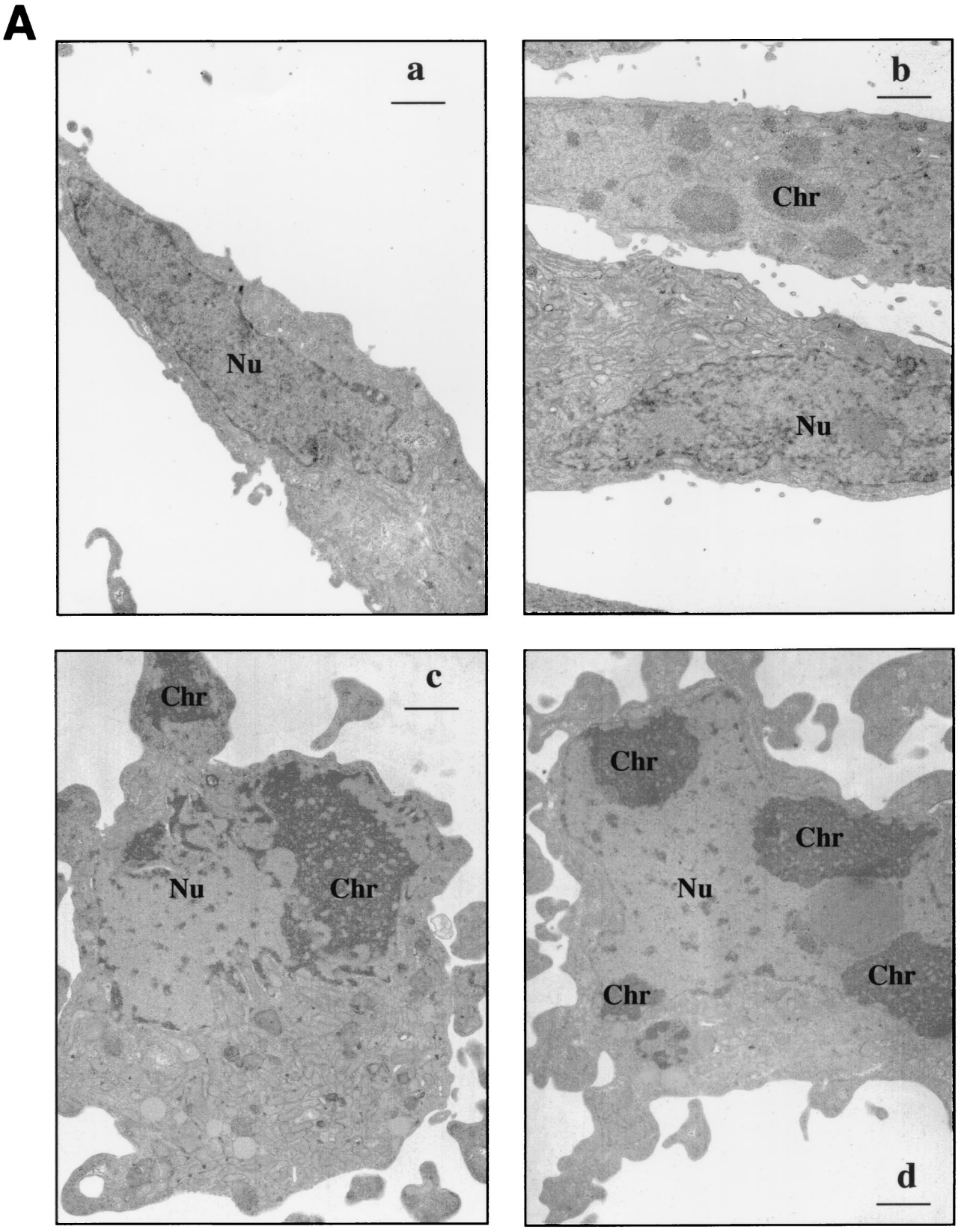

FIG. 2

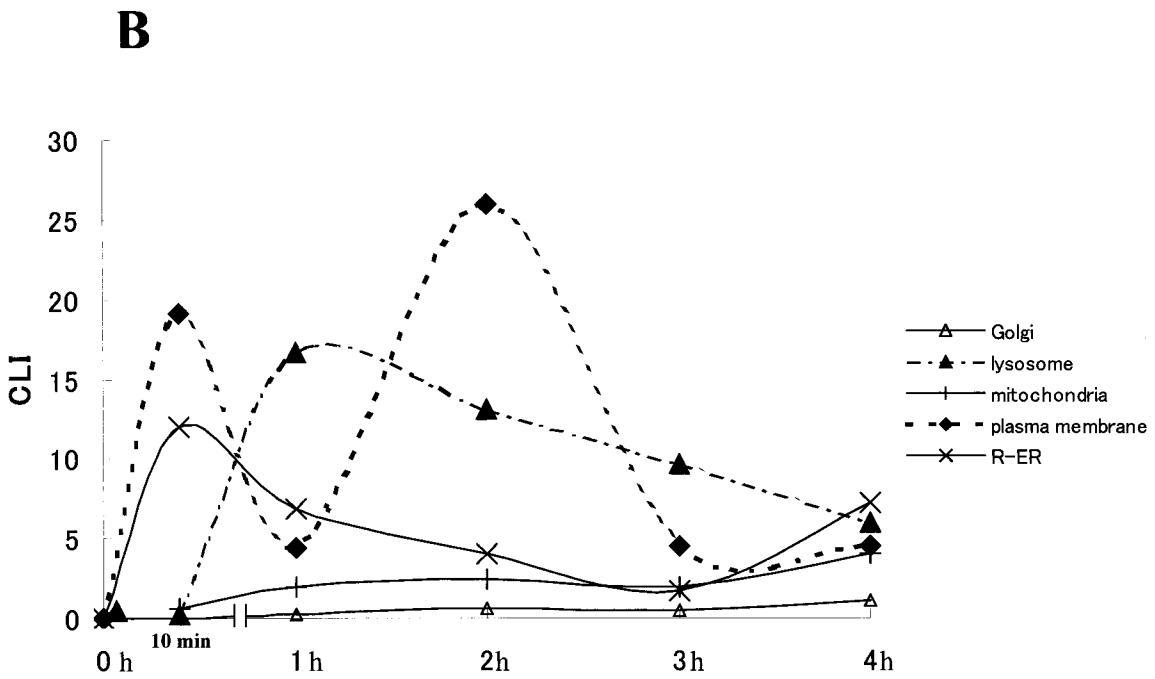

FIG. 2. (A) Morphology of Stx2-treated HeLa cells. (a) Control. Note the fibroblastic appearance typical of untreated cells with the characteristic oblong euchromatic nucleus (Nu). (b through d) Cells treated with Stx2 (10 ng/ml) for 4 h. (b) The lower cell has a morphology similar to that of a control cell. In contrast, note that in the upper cell the chromatin (Chr) has started to aggregate in fine granular masses, yet the cell maintains its fibroblastic shape. (c) The cell has begun to round up, and the cytoplasm has started to bleb. Within the nucleus, note the fine granular chromatin concentrated in the periphery of the nucleus associated with the nuclear envelope. Also evident is a fragment of the chromatin associated with a cytoplasmic bleb in the right-hand corner of the micrograph. (d) The fine granular masses of chromatin are associated with the nuclear envelope. The cell shown is rounded, and the cytoplasm has begun to bleb. The morphology shown in panels c and d was characteristic of >50% of the cells viewed in samples 4 h after treatment with Stx2. Bars, 1 μm; final magnification, ×7,500. (B) Stx2 trafficking in HeLa cells analyzed by immunogold electron microscopy. Stx2A distribution was quantified in cytoplasmic compartments such as the Golgi apparatus, lysosome, mitochondria, plasma membrane, and R-ER.

sucrose containing 4.0% paraformaldehyde and 0.5% glutaraldehyde). All subsequent steps were performed as described above. After the blocks were hardened, ultrathin sections were cut and picked up onto 300-mesh nickel grids. A postembedding immunostaining protocol was used to label Stx with gold (39). Briefly, immunogold labeling was initiated by incubating the grids with the appropriately diluted primary antibody (anti-Stx2A monoclonal antibody) for 60 min. After the three washes between steps, the grids were incubated for 60 min with droplets of affinity-purified, biotinylated goat anti-mouse secondary antibody (IgG fraction, diluted to 50 μg/ml; KPL, Gaithersburg, Md.). After another wash, the grids were finally incubated with droplets of streptavidin-gold. The immunolabeled grids were next washed with droplets of double-distilled water, stained for 10 min at 23°C with 2% uranyl acetate (aqueous), and viewed as described above. Controls included (i) a sample using an irrelevant primary antibody, (ii) a sample in which bicarbonate buffer was used in place of the primary antibody, and (iii) a sample in which bicarbonate buffer replaced both the primary and the secondary antibody. The comparative labeling index (CLI) value was determined by multiplying the relative labeling index (RLI) value by the labeling density (37). The CLI is the best value for making between-group comparisons, whereas the RLI is best for making within-group comparisons.

Analysis of DNA fragmentation. HeLa cells (10^6) grown in 6-well culture plates were treated with Stx1 (0.1 to 10 ng/ml) for 2 or 4 h. Cells were harvested for DNA extraction with a DNA extraction kit (Sepa Gene; Sankou-Jyunyaku Co., Ltd.). For quantitation of DNA fragmentation, following stimulation with Stx1 (10 ng/ml), HeLa cells (10^6) were incubated in RPMI-1640 in 6-well Costar plates for different times. Cells were harvested by centrifugation at 200 × *g* for 10 min. Pellets were lysed with 0.3 ml of hypotonic lysing buffer (10 mM Tris–10 mM EDTA) containing 0.5% Triton X-100, and lysates were centrifuged at 13,000 × *g* for 10 min to separate intact from fragmented chromatin. The supernatant, containing DNA fragments, was placed in a separate microcentrifuge tube, and both pellet and supernatant were treated at 4°C for 30 min with 1 N perchloric acid. Precipitates were sedimented at 13,000 × *g* for 20 min. DNA precipitates were hydrolyzed by heating to 70°C for 10 min in 0.15 ml of 1 N perchloric acid (and quantitated by using a modification of the diphenylamine method of Burton [8]).

In situ DNA fragmentation was investigated by the terminal deoxynucleotidyltransferase-mediated dUTP-biotin nick end labeling (TUNEL) method by use of the Apop Tag peroxidase in situ apoptosis detection kit (Intergen Company, Purchase, N.Y.). To obtain an accurate total count of apoptotic HeLa cells with in situ DNA fragmentation, cells were cultured overnight in Lab-Tec slide chambers and centrifuged (Cytospin; Thermo Shandon, Inc., Pittsburgh, Pa.) prior to analysis.

Flow cytometric analysis of changes in Δψ. HeLa cells were pretreated with brefeldin A (5 μg/ml) for 30 min, followed by addition of Stx1 (10 ng/ml). At 1, 2, 3, or 4 h after addition of Stx1, the cells were harvested as described above, washed twice in phosphate-buffered saline (PBS), resuspended at a concentration of 5×10^5 cells/ml in RPMI 1640 medium with 10% FCS containing 100 μg of JC-1/ml, and incubated at 37°C for 10 min. Cells were then washed twice in cold PBS, and samples were analyzed. Cell fluorescence was recorded using a FACScan cytometer (Becton Dickinson, San Jose, Calif.) equipped with a 488-nm argon laser (FL1) and a 568-nm argon-krypton laser (FL2). JC-1 fluorescence was analyzed on the FL1 and FL2 channels for detection of the dye monomer and J-aggregate forms, respectively. HeLa cells were pretreated with caspase inhibitors to determine their effects on Stx1-induced changes in mitochondrial membrane potential (Δψ).

HeLa cells were pretreated with 20 μM general caspase inhibitor or caspase-8 inhibitor for 1 h at 37°C before stimulation of cells with Stx1 (10 ng/ml) followed at 4 h by flow cytometric analysis of changes in Δψ, as described above.

Determination of caspase enzymatic activity. After HeLa cells (10^7) were treated with Stx1 (10 ng/ml), they were washed with ice-cold PBS and lysed with an ice-cold buffer solution containing 50 mM KCl, 50 mM PIPES (pH 7.0), 10 mM EGTA (pH 7.0), 2 mM $MgCl_2$, 20 μM cytochalasin B, 10 mM dithiothreitol (DTT), 1 mM phenylmethylsulfonyl fluoride, 1 μg of pepstatin/ml, 1 μg of

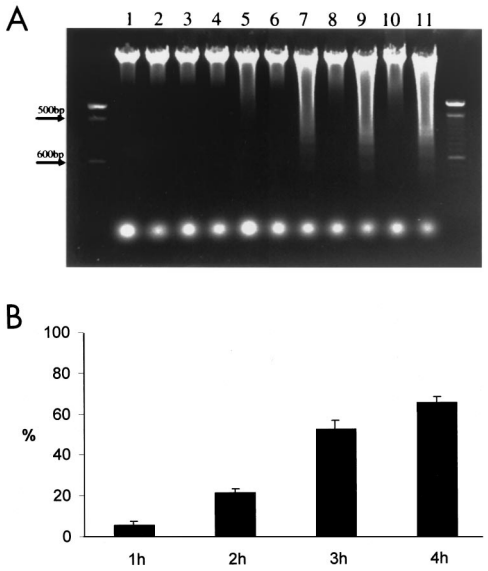

FIG. 3. (A) Gel electrophoretic analysis of HeLa cell DNA fragmentation. At 2 or 4 h after incubation of HeLa cells with Stx1 (100 pg/ml to 100 ng/ml), DNA fragmentation analysis was performed as described in Materials and Methods. Lane 1, control without Stx1; lanes 2 through 11, Stx1 treatment. Cells were treated with Stx1 at 10 pg/ml (lanes 2 and 3), 100 pg/ml (lanes 4 and 5), 1 ng/ml (lanes 6 and 7), 10 ng/ml (lanes 8 and 9), or 100 ng/ml (lanes 10 and 11) and were analyzed at 2 h (lanes 2, 4, 6, 8, and 10) or 4 h (lanes 3, 5, 7, 9, and 11) after treatment. (B) Quantitation of Stx1-induced DNA fragmentation. The percent DNA fragmentation per total cellular DNA was determined by the Burton method to be 5.37% ± 1.75% at 1 h, 21.15% ± 1.73% at 2 h, 51.91% ± 4.43% at 3 h, and 64.62% ± 3.03% at 4 h after treatment of HeLa cells with Stx1 (10 ng/ml).

antipain/ml, 1 μg of leupeptin/ml, and 1 μg of chymostatin/ml. The samples were frozen and thawed five times by using liquid nitrogen, and cell lysates were centrifuged to obtain supernatants which were used for the assay of caspase proteolytic activity. Caspase proteolytic activity was monitored by using the fluorogenic AFC-peptide substrate in caspase reaction buffer {100 mM HEPES, 10% sucrose, 0.1% 3-[(3-cholamidopropyl)-dimethylammonio]-1-propanesulfonate [CHAPS], 10 mM DTT, 1 mM phenylmethylsulfonyl fluoride, 1 μg of pepstatin/ml, 1 μg of antipain/ml, 1 μg of leupeptin/ml, 1 μg of chymostatin/ml}. Caspase cleaved AFC from the peptide and released free AFC, which was detected in a kinetic microplate fluorescence reader (FL600; BIO-TEC Instrument, Inc., Winooski, Vt.) at excitation and emission wavelengths of 380 and 530 nm, respectively. Measurements to determine the linearity of the enzymatic reaction were made at 5-min intervals over a 1-h period. Total cell protein was measured with Coomassie plus-200 reagent (Pierce Chemical Co., Rockford, Ill.) at 590 nm in a microplate reader. Caspase activity was expressed as picomoles of AFC liberated per milligram of protein per minute. Alternatively, HeLa cells were pretreated with 20 μM inhibitor of caspase-3, -6, or -8 for 1 h at 37°C before stimulation of cells with Stx1 (10 ng/ml). Caspase-3 proteolytic activity was measured as described above at 3 h after addition of Stx1.

Effects of brefeldin A and caspase inhibitors on apoptosis induced by Stx1. HeLa cells were pretreated with different concentrations of brefeldin A for 1 h at 37° before stimulation with Stx1 (10 ng/ml). DNA extracts were prepared as described above. In some cases, HeLa cells were pretreated with caspase inhibitor (20 μM) for 1 h at 37°C before stimulation with Stx1 and Stx2 (10 ng/ml).

Immunoblotting of HeLa cell proteins. Cytochrome *c* levels were analyzed as described by Heibein et al. (18). Full-length (inactive) and protease-cleaved (active) fragments were detected by Western blotting as described by Bitko and Barik (6). Briefly, HeLa cells (2×10^7 cells/10 ml in RPMI with 10% heat-inactivated FCS) were treated with Stx1 (10 ng/ml) for the time indicated. Cells were washed twice with cold PBS and resuspended in 100 μl of digitonin lysis buffer (75 mM NaCl, 1 mM NaH_2PO_4, 8 mM Na_2HPO_4, 250 mM sucrose, 190 μg of digitonin/ml) or caspase lysis buffer (50 mM Tris HCl [pH 8.0], 50 mM NaCl, 0.1 mM EDTA, 1% Tween 20, 1 mM DTT, and 1 mM each leupeptin, aprotinin, and phenylmethylsulfonyl fluoride). Digitonin is a weak nonionic detergent that, at low concentrations, selectively renders the plasma membrane permeable, releasing cytosolic components from cells but leaving other organelles intact (1). After 5 min on ice, the cells were spun for 5 min at 15,000 × *g* at 4°C in a microcentrifuge. Supernatants were transferred to fresh tubes. Aliquots (10 μl) of supernatants for each sample were added to 20 μl of Laemmli buffer (Bio-Rad Laboratories, Hercules, Calif.) and boiled at 92°C for 2 min. Western immunoblotting was carried out using the ECL detection system (Amersham Pharmacia Biotech, Little Chalfont, Buckinghamshire, England). Protein expression of 15-kDa Bid was quantitated by using densitometry and ImageQuant, version 5.2, software.

Flow cytometric analysis of cell surface Fas expression and reverse transcription-PCR (RT-PCR) analysis of cytokines. HeLa cells were harvested after incubation for 45 min at 4°C with 2 ml of PBS containing 0.1% EDTA. After a wash with PBS at 4°C, the cells were incubated for 1 h at 4°C in 50 μl of FACS buffer (PBS containing 2.5% fetal bovine serum and 0.1% NaN_3) containing 20 μl of a PE-conjugated mouse monoclonal antibody to human Fas. Cells were washed three times with FACS buffer and analyzed with a FACScan cytometer (Becton Dickinson).

For RT-PCR of cytokines, total RNA was extracted with ISOGEN (Nippon Gene, Tokyo, Japan) according to the protocol of the supplier. cDNA was synthesized by incubating 1 mg of cellular RNA in a 20-ml reaction mixture containing 50 mM Tris-HCl (pH 8.3), 75 mM KCl, 8 mM $MgCl_2$, 10 mM DTT, 20 ng of a random primer (Takara, Otsu, Japan)/ml, 1 mM each deoxynucleoside triphosphate, RNase inhibitor, and RAV-2 reverse transcriptase (Takara) for 60 min at 37°C. PCR was carried out using TaKaRa *Taq* DNA polymerase (Takara) according to the recommendations of the supplier. Primer sequences were as follows: for TNF-α, the sense primer was 5′-ATGAGCACAGAAAGCATGATCCGC-3′ and the antisense primer was 5′-CCAAAGTAGACCTGCCCGGACTC-3′; for interleukin1-β (IL-1β), the sense primer was 5′-TCC TTG TGC AAG TGT CTG AA-3′ and the antisense primer was 5′-GAG AGG TGC TGA TGT ACC AG-3′; for β-actin, the sense primer was 5′-GTGGGCCGCTCTAGGCACCAA-3′ and the antisense primer was 5′-CTCTTTGATGTCACGCACGATTTC-3′. The sizes of the PCR products for TNF-α, IL-1β, and β-actin were determined to be 692, 752, and 360 bp, respectively.

RESULTS

Stx1 induction of apoptosis in HeLa cells. Apoptotic, TUNEL-positive cells became detached from the substratum but could be readily captured with a brief Cytospin centrifugation prior to staining. By use of this approach, Stx1 treatment (10 ng/ml) for 4 h resulted in 64% TUNEL-positive cells (Fig. 1B) versus less than 1% TUNEL-positive control cells (in the absence of Stx1) (Fig. 1A).

Stx2-induced apoptosis was also clearly evident by electron microscopy. Figure 2A shows untreated control HeLa cells with a typical fibroblastic appearance and a characteristic oblong euchromatic nucleus (Fig. 2Aa) and HeLa cells treated with Stx2 (10 ng/ml) for 4 h (Fig. 2Ab). The lower cell in Fig. 2Ab has a morphology similar to that of the control. In contrast, in the upper cell, the chromatin has begun to aggregate in fine granular masses, yet the cell maintains the fibroblastic shape. In Fig. 2Ac, a 4-h-Stx2-treated HeLa cell has begun to round up and the cytoplasm has started to bleb. Within the nucleus, fine granular chromatin is concentrated in the periphery of the nucleus associated with the nuclear envelope. A fragment of the chromatin is associated with a cytoplasmic bleb. In Fig. 2Ad also, fine granular masses of chromatin are associated with the nuclear envelope. Note that the cell shown is rounded and the cytoplasm has begun to bleb. The morphology shown in Fig 2Ac and d was characteristic of >50% of the cells viewed in samples 4 h after treatment with Stx2.

This apoptotic effect of Stx1 on HeLa cells was also confirmed by analysis of DNA fragmentation in HeLa cells treated with Stx1 (Fig. 3A). A minimum 3-h exposure to 10 ng of

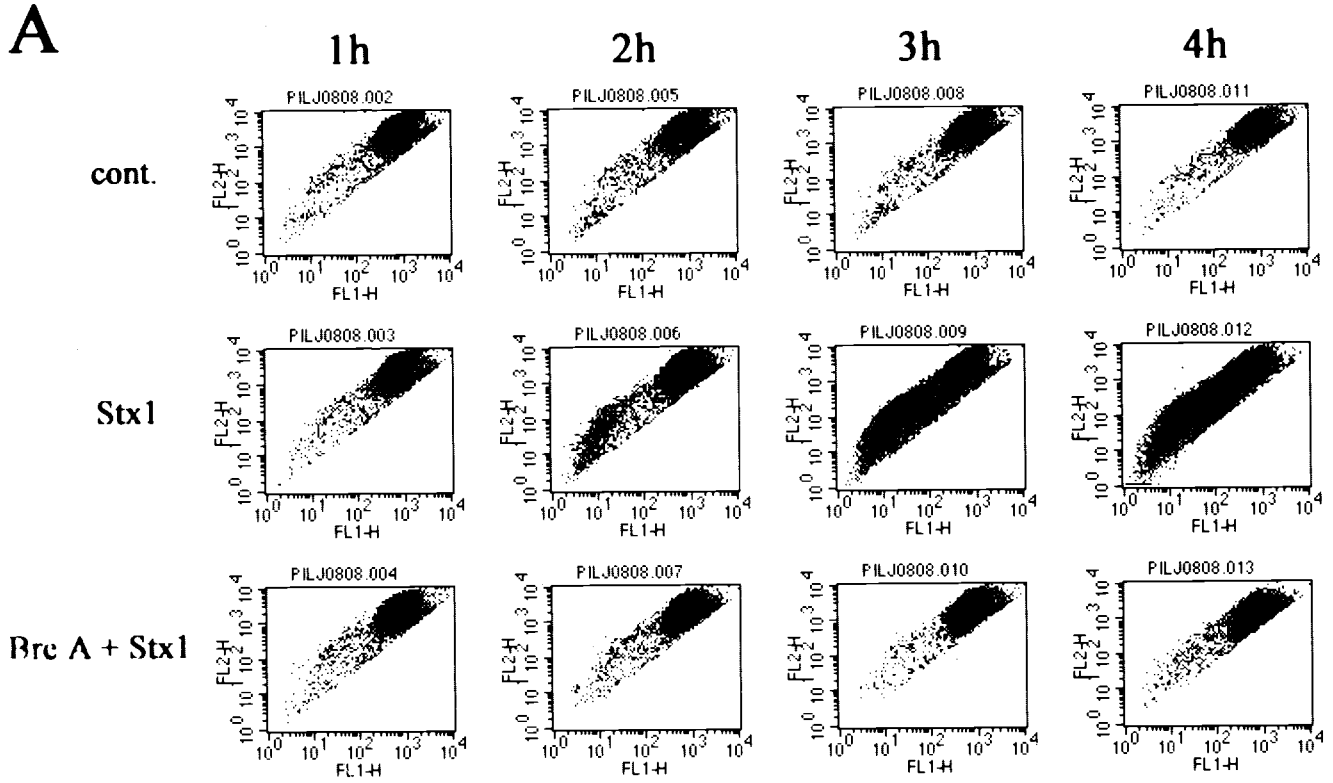

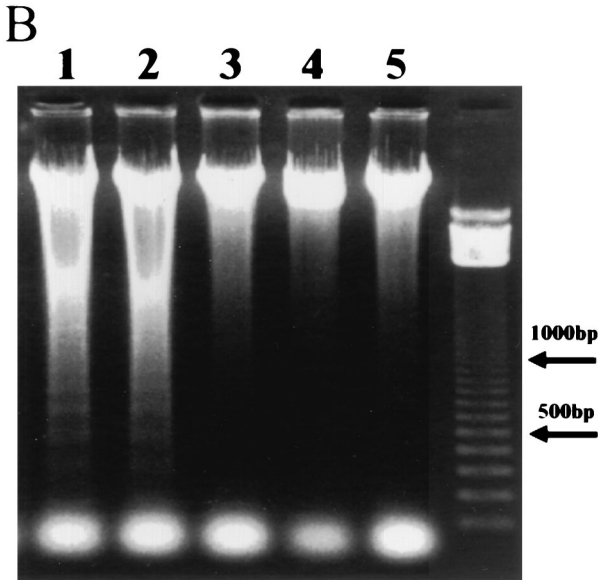

FIG. 4. (A) Reduction in $\Delta\psi$ after incubation of HeLa cells with Stx1. $\Delta\psi$ was determined by flow cytometry with the reagent JC-1 as described in Materials and Methods. A decrease in $\Delta\psi$ was associated with a shift of reactive cells toward the lower left quadrant at 3 and 4 h after incubation with Stx1. cont., cells treated without Stx1; Stx1, cells treated with Stx1 (10 ng/ml); Bre A + Stx1; cells pretreated for 1 h with brefeldin A (5 μg/ml) followed by treatment with Stx1 (10 ng/ml).(B) Effects of brefeldin A on apoptosis induced by Stx1 in HeLa cells. Cells either were not pretreated or were preincubated with brefeldin A for 1 h before treatment with Stx1 (10 ng/ml) for 4 h (lanes 1 to 4). DNA fragmentation was then analyzed as described in Materials and Methods. Lane 1, 100 ng of brefeldin A/ml; lane 2, 500 ng/ml; lane 3, 5 μg/ml; lane 4, 50 μg/ml; lane 5, 50 μg of brefeldin A/ml without Stx1.

Stx1/ml was required for apoptosis of HeLa cells. Fragmented DNA was quantified by the Burton method (8) and expressed as percent DNA fragmentation per total cellular DNA. Calculated values for HeLa cells treated with 10 ng of Stx1/ml were 0.07% at 1 h, 0.26% at 2 h, 33.6% at 3 h, and 43.4% at 4 h (Fig. 3B).

Intracellular trafficking of active Stx1A is required for induction of apoptosis. Additional data indicated that internalization and processing of Stx1 holotoxin within HeLa cells was required for the apoptotic response. A brief preincubation of HeLa cells with the Golgi inhibitor brefeldin A (5 μg/ml) prevented the apoptotic effects (mitochondrial damage [Fig. 4A] and DNA fragmentation [Fig. 4B]) of Stx1 (10 ng/ml). Brefeldin A alone had no effect on the cells under these conditions. Thus, movement of Stx2 within HeLa cells was examined by immunogold detection of the Stx2 A subunit. Immunogold electron microscopic analysis of Stx2-treated cells showed that Stx2A was distributed in cytoplasmic compartments such as the Golgi apparatus, mitochondria, nucleus, and rough endoplasmic reticulum (R-ER) (Fig. 2B). The CLI quantitative value of Stx2A in the R-ER reached a maximum at 10 min after addition of Stx2. At 1 h and beyond, the mitochondrial CLI value increased as the CLI value for the R-ER was decreasing. CLI values for the Golgi apparatus and mitochondria were increased minimally over the entire 4-h period, but the CLI values of lysosomes reached a peak at 1 h, and the CLI value of plasma exhibited two peaks at 10 min and 2 h.

Enzymatically active holotoxin is required for Stx1 induc-

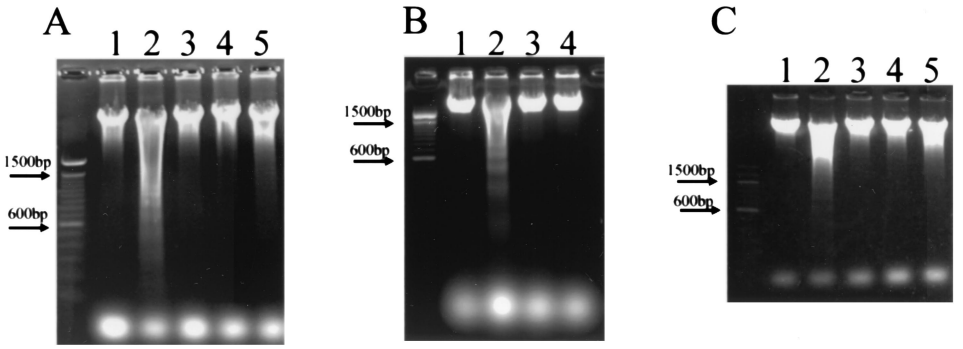

FIG. 5. Effects of the Stx1 B subunit (A), the CD77 MAb (B), and the Stx2 E166D mutant (C) on DNA fragmentation in HeLa cells. Cells were incubated for 4 h and analyzed for DNA fragmentation as described in Materials and Methods. In all panels, lane 1 contains no Stx1 and lane 2 contains Stx1 at 10 ng/ml. (A) Lanes 3 to 5, Stx1B at 78.5 ng/ml (lane 3), 785 ng/ml (lane 4), or 3.96 μg/ml (lane 5). (B) Lanes 3 and 4, CD77 MAb at 0.5 or 5 μg/ml, respectively. (C) Lanes 3 to 5, Stx2 E166D at 40 ng/ml (lane 3), 400 ng/ml (lane 4), or 4 μg/ml (lane 5).

tion of apoptosis. Additional data were gathered to determine which subunit of Stx2, Stx2A or Stx2B, was responsible for the apoptotic response. The Stx2 E166D enzymatic site mutant did not cause apoptosis when incubated with HeLa cells (Fig. 5C). In addition, the purified Stx1 B subunit, active in binding to the Stx1 receptor but lacking the enzymatic A subunit, was incapable of causing DNA fragmentation (Fig. 5A). This was observed even when the Stx1 B subunit was present at 10 to 100 times the molar concentration of intact Stx1 required to cause apoptosis in these cells. Finally, exposure of HeLa cells to a monoclonal antibody specific for the Stx1 receptor CD77 did not lead to apoptosis (Fig. 5B). These results indicate that occupation of the toxin receptor alone is insufficient for the apoptotic response and that apoptosis required an enzymatically active A subunit of the toxin.

Caspase activity is required for Stx1-induced apoptosis. Caspase enzymes, which are major components of an apoptotic cascade, were examined in HeLa cells exposed to Stx1 and Stx2. By use of fluorescent peptide substrates for individual caspases, it was noted that Stx1 caused an increase in the enzymatic activity of caspases 3, 6, 8, and 9 (Fig. 6A). Activities for these caspases peaked at 3 h and returned to baseline at 4 or 5 h. Further evidence that Stx1 caused an increase in the enzymatic activity of caspases 3, 6, 8, and 9 was provided by immunoblot analysis. Conversion of caspases 3, 8, and 9 from the inactive procaspase to the cleaved, active caspase is displayed in Fig. 7. In addition, the procaspase form of caspase-6 decreased in a time-dependent manner, and as a result, lamin A, a specific enzyme, was cleaved (Fig. 7). Further data supporting a role for caspases 3, 6, and 8 in Stx1-induced apoptosis are displayed in Fig. 6B, where inhibitors of caspases 3, 6, and 8 are shown to effectively block the apoptotic cascade and DNA fragmentation. However, inhibitors of caspases 1, 2, and 9 did not prevent apoptosis and DNA fragmentation (Fig. 6B and C).

Stx1-induced activation of the mitochondrial pathway of apoptosis. Because caspase-8 activity is known to initiate the mitochondrial pathway of apoptosis in many cell types, we examined the individual factors in this pathway after exposure of HeLa cells to Stx1. Indeed, the mitochondrial factor Bid was converted from an inactive 26-kDa form to an active 15-kDa agent capable of disrupting the mitochondrial outer membrane (Fig. 7). Analysis of changes in $\Delta\psi$ by flow cytometry revealed that the population of JC-1-positive cells, those cells with a decreased $\Delta\psi$, increased following exposure to Stx1 (Fig. 4A). This was indicated by a shift in population from upper right to lower left at 2, 3, and 4 h compared with the pattern for control cells without Stx1. As an indicator of mitochondrial damage, leakage of cytochrome *c* from mitochondria into the cytoplasm was observed after incubation of HeLa cells with Stx1 (Fig. 7). Cytochrome *c* typically forms a multimeric complex with dATP and Apaf-1, resulting in activation of caspase-9. Evidence that this happened in Stx1-treated HeLa cells is shown in Fig. 6A and 7, where this formation of active caspase-9 occurs. Thus, a complete set of apoptosis-related mitochondrial factors was revealed after Stx1 treatment of HeLa cells. However, and unexpectedly, levels of XIAP, a potent inhibitor of active caspase-9, increased in a Stx1-dependent manner (Fig. 7). These data suggested that caspase-9 activity was not involved in Stx1-induced apoptosis of HeLa cells. In support of this concept are data showing that an inhibitor of caspase-9 could not prevent Stx1- or Stx2-induced DNA fragmentation in HeLa cells (Fig. 6B and C).

Nonetheless, different inhibitors of Stx1-induced apoptosis were also able to indirectly prevent the Stx1-dependent decrease in $\Delta\psi$. A brief preincubation of HeLa cells with brefeldin A (5 μg/ml) that prevented DNA fragmentation (Fig. 4B), described above, also blocked the Stx1-specific decrease in $\Delta\psi$ (Fig. 4A). Thus, mitochondrial (Fig. 4A) and nuclear changes, i.e., DNA fragmentation (Fig. 4B), typical of apoptosis both required internalization and processing of Stx1 in HeLa cells. It should be noted that inhibition of caspase-8 also prevented the Stx1-dependent decrease in $\Delta\psi$ (Fig. 8). Together, these results demonstrate that activated caspase-8 might cleave downstream caspase-3 in one direction and also cleave Bid in the mitochondrial direction. However, only the former pathway may be functional for apoptosis in Stx1-treated HeLa cells.

Effects of pretreatment with caspase-3, -6, or -8 inhibitor on caspase-3 cleavage activity induced by Stx1. Capase-3 inhibitor, caspase-6 inhibitor, and capase-8 inhibitor blocked the increase in caspase-3 enzyme activity (Fig. 9). It should be noted that inhibitors of caspase-6 and -8 individually are much less inhibitory toward caspase-3.

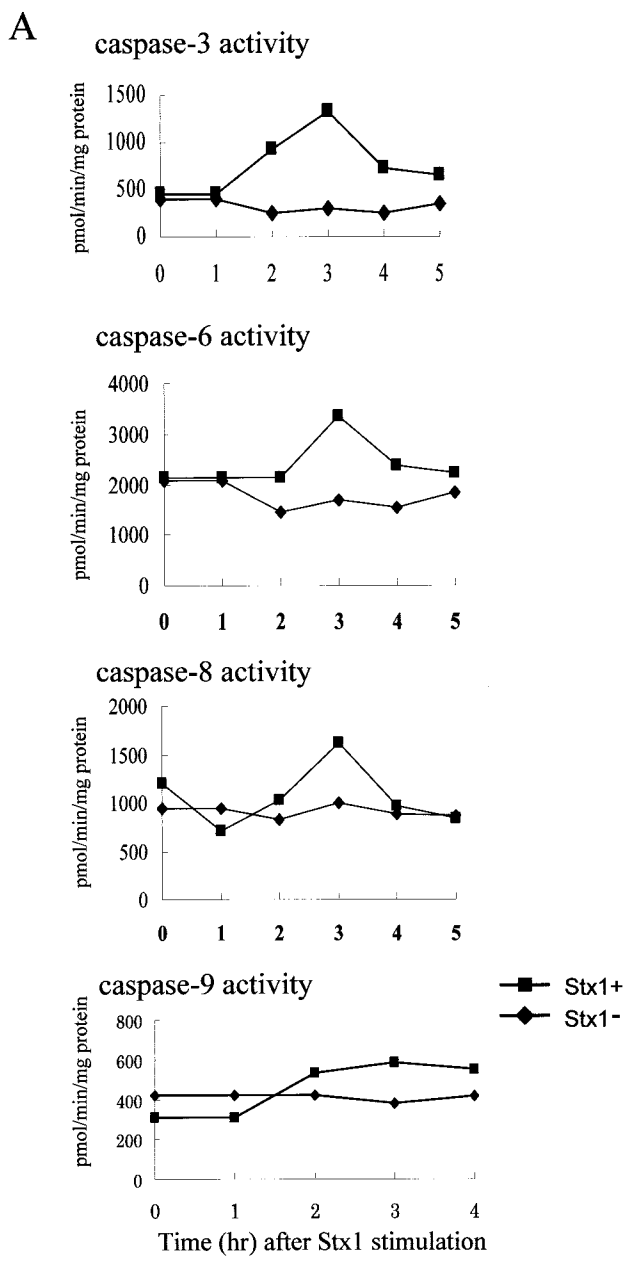

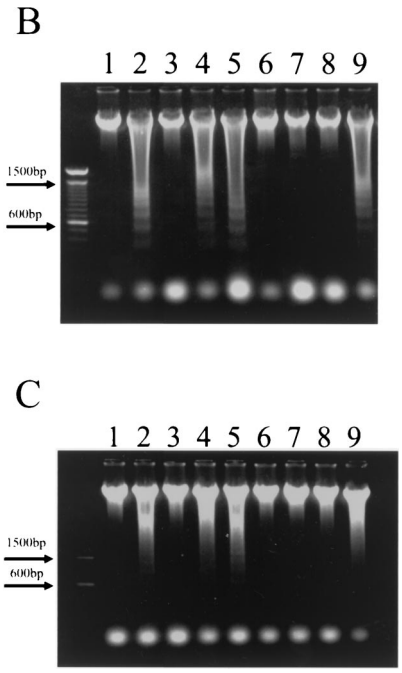

FIG. 6. (A) Effects of Stx1 on caspase enzymatic activities in HeLa cells. Cells were incubated without or with Stx1(10 ng/ml) for the times indicated, and activities of caspases 3, 6, 8, and 9 were monitored with fluorescent substrates in microtiter plate format as described in Materials and Methods. (B) Effects of caspase inhibitors on Stx1-induced apoptosis in HeLa cells. Cells were preincubated with caspase inhibitors for 1 h, followed by incubation with Stx1 (10 ng/ml) for 4 h, where indicated. All caspase inhibitors were used at 20 μM. Lane1, no Stx1 or caspase inhibitor; lane 2, Stx1 only; lane 3, Stx1 plus general caspase inhibitor (Z-VAD-fmk); lane 4, Stx1 plus caspase-1 inhibitor (Z-YVAD-fmk); lane5, Stx1 plus caspase-2 inhibitor (Z-VDVAD-fmk); lane 6, Stx1 plus caspase-3 inhibitor (Z-DEVD-fmk); lane 7, Stx1 plus caspase-6 inhibitor (Z-VEID-fmk); lane 8, Stx1 plus caspase-8 inhibitor (Z-IETD-fmk); lane 9, Stx1 plus caspase-9 inhibitor (Z-LEHD-fmk). (C) Effects of caspase inhibitors on Stx2-induced apoptosis in HeLa cells. All caspase inhibitors were used at 20 μM. Lane1, no Stx2 (10 ng/ml) or caspase inhibitor; lane 2, Stx2 only; lane 3, Stx2 plus general caspase inhibitor (Z-VAD-fmk); lane 4, Stx2 plus caspase-1 inhibitor (Z-YVAD-fmk); lane5, Stx2 plus caspase-2 inhibitor (Z-VDVAD-fmk); lane 6, Stx2 plus caspase-3 inhibitor (Z-DEVD-fmk); lane 7, Stx2 plus caspase-6 inhibitor (Z-VEID-fmk); lane 8, Stx2 plus caspase-8 inhibitor (Z-IETD-fmk); lane 9, Stx2 plus caspase-9 inhibitor (Z-LEHD-fmk).

Stx1 did not induce Fas expression on the cell surface or increase TNF-α or IL-1β mRNA levels. It was observed that Stx1-treated apoptotic cells did not react with Fas, indicating a lack of Fas expression on the cell surfaces. After stimulation by a 4-h incubation with Stx1 (10 ng/ml), Fas expression was decreased, with a mean fluorescence intensity value of 141 in control (no toxin) cells versus 60 in Stx1-stimulated cells. Addition of Stx1 (10 ng/ml) to HeLa cells did not increase TNF-α or IL-1β mRNA (data not shown) levels, as determined by RT-PCR (data not shown).

Stx1-dependent apoptosis in HeLa cells. In summary, the results described above suggest that Stx1 and Stx2 cause apoptosis of HeLa cells according to the pathway scheme in Fig. 10.

DISCUSSION

The results presented show that subnanomolar concentrations of Stx1 cause apoptosis of HeLa cells within 4 h and that the apoptosis (i) is dependent on induction of caspases 3, 6, and 8, (ii) requires intracellular trafficking of enzymatically active holotoxin, (iii) is not initiated by the Stx2 B subunit alone, (iv) is not facilitated by an activated mitochondrial pathway of apoptosis, and (v) involves activation of caspase-3 by caspase-8. Stx-induced apoptosis was demonstrated by several methods including DNA fragmentation, TUNEL staining of whole cells, and electron microscopic confirmation of nuclear disassembly. The apoptotic pathway described appears to be

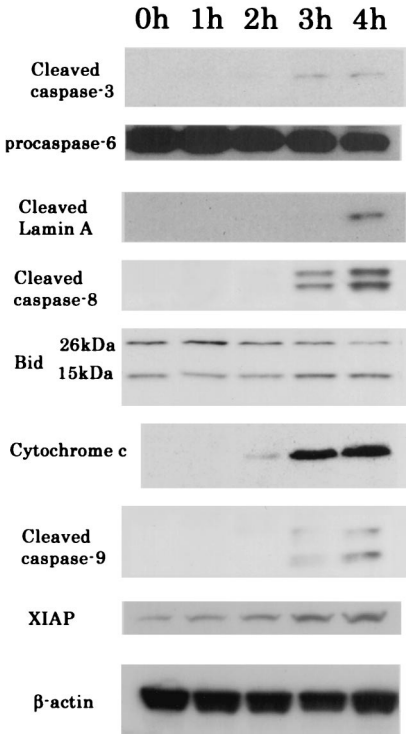

FIG. 7. Stx2 induction of HeLa cell apoptosis-related factors. Cells were removed at the indicated times and analyzed by immunoblotting. Caspase-3, caspase-6, caspase-8, and caspase-9 were cleaved, and cleaved lamin A and Bid (15 kDa) are shown. After treatment of HeLa cells with Stx1 (10 ng/ml), levels of activated Bid (15 kDa), measured by densitometry and compared with control levels (at 0 h), were increased 1.8- and 1.7-fold at 3 and 4 h, respectively. Cytochrome *c* was detected in the cytosolic fraction at 3 to 4 h after treatment with Stx1 (10 ng/ml). Endogenous XIAP levels were increased in a time-dependent manner. β-Actin was used as an internal loading control for equal amounts of protein.

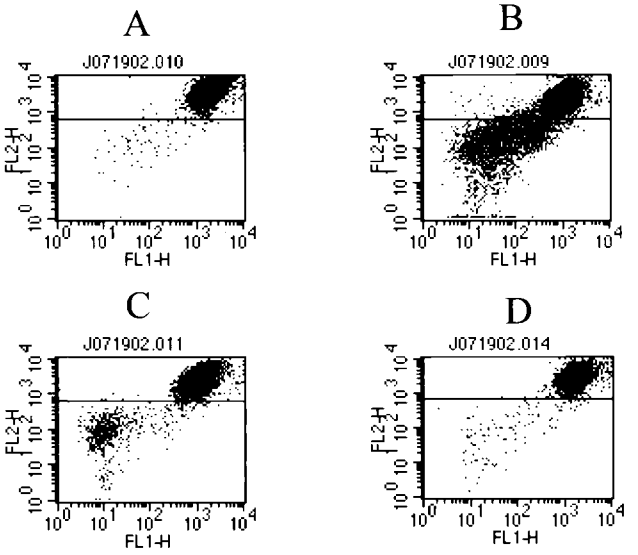

FIG. 8. Effects of caspase inhibitors on Stx1-dependent mitochondrial damage. HeLa cells were preincubated with caspase inhibitors (20 μM) for 1 h followed by incubation with Stx1 (10 ng/ml) for 4 h. $\Delta\Psi$ was then measured as described in Materials and Methods. (A) Control without Stx1. The percentage of the area below the line is 0.97. (B) Stx1. The percentage of the area below the line is 29.9. (C) Stx1 plus pretreatment with general caspase inhibitor (Z-VAD-fmk). The percentage of the area below the line is 5.9. (D) Stx1 plus caspase-8 inhibitor (Z-DEVD-fmk). The percentage of the area below the line is 1.55.

activated by Stx1 and Stx2 in HeLa cells and represents the first report of such a Stx-induced pathway.

These data differ from the findings of Nakagawa et al. (41), who reported that apoptosis or necrosis was induced in HeLa/C4 cells by internal expression of the Stx1 B or A subunit, respectively, following transfection of the cells with the individual genes for these subunits. They observed that Stx1B generated intracellularly caused apoptosis that was dependent on caspases 1 and 3. Our results clearly show that extracellular Stx1B did not induce DNA fragmentation in HeLa cells and that Stx1 holotoxin-induced apoptosis was dependent on caspases 3, 6, and 8 but not on caspases 1 and 3. The high specificity of inhibitors of caspase-6 or -8 versus caspase-3 allowed us to determine that caspases 6 and 8 were upstream of caspase 3 (Fig. 9). However, the cross-reactivity of caspase-6 and -8 inhibitors prevented determination of the relative placement in the pathway of these two caspases. Thus, we have placed caspases 6 and 8 at an equal level (Fig. 10). The data leading to our conclusions were derived from multiple and different assays.

Our final scheme (Fig. 10) depicts two apoptotic pathways, from caspase-6 and caspase-8: (i) caspase-8 activation of caspase-3, leading to DNA fragmentation, and (ii) caspase-6 activation of lamin A, leading to nuclear disassembly and chromatin condensation. The former pathway has been reported for BL cells, where Stx1-induced apoptosis was prevented by inhibitors of caspases 3 and 8, and where it was concluded that caspase-8 was located upstream of caspase-3 in the caspase

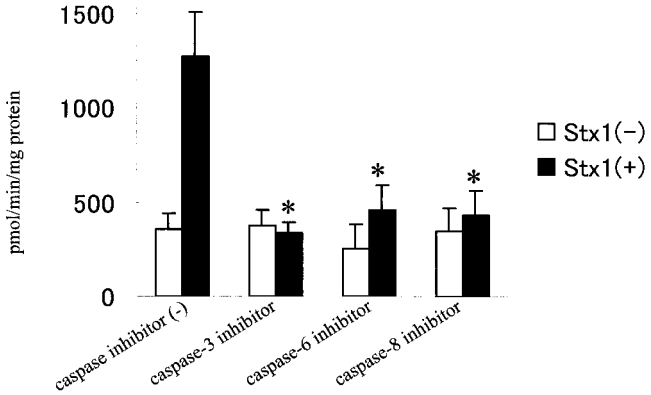

FIG. 9. Effects of caspase inhibitors on caspase-3 activity induced by Stx1. HeLa cells were preincubated for 1 h with specific inhibitors (20 μM) of caspase-3, -6, or -8 followed by a second incubation without or with Stx1 (10 ng/ml) for 3 h. Caspase-3 enzymatic activity was then measured with a specific fluorescent substrate in a microtiter plate format as described in Materials and Methods. Inhibitors were capase-3 inhibitor (Z-DEVD-fmk), caspase-6 inhibitor (Z-VEID-fmk), and capase-8 inhibitor (Z-IETD-fmk). Comparisons were made between no-pretreatment and caspase-inhibitor-pretreatment groups with Stx1 (*, $P < 0.05$, *t* test).

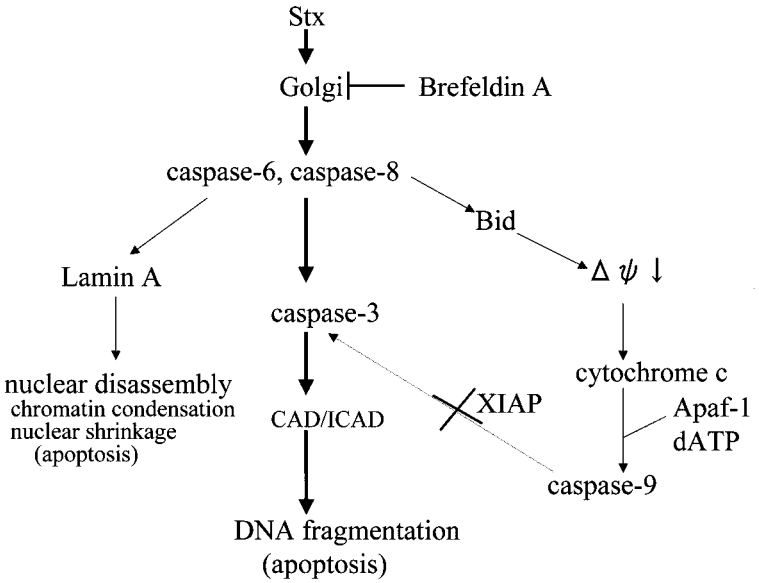

FIG. 10. A proposed cascade of apoptosis induced by Stx1 and Stx2 in HeLa cells.

cascade (27). Our results show a similar relationship of caspases 8 and 3 in Stx1-treated HeLa cells. The caspase-6 pathway has been reported for other, non-Stx apoptotic systems (47, 51). Allsopp et al. reported that active caspase-6 is capable of processing and activating procaspase-3 in cellular extracts prepared from nonapoptotic cerebellar granule cells (2). We could find active caspase-6 protein for Western blots (data not shown), and we also depended on proteolytic cleavage of lamin A, a specific enzyme for caspase-6. These caspase-6 results were confirmed by a decrease in procaspase 6 levels, as observed in Western blotting.

The requirement for intracellular trafficking of enzymatically active Stx2 was demonstrated with the Golgi apparatus inhibitor brefeldin A and with a Stx2 holotoxin that has a single amino acid change in the enzymatic site of the Stx2 A subunit. In both cases, apoptosis did not occur. Immunogold electron microscopic analysis of intracellular internalized Stx2 holotoxin clearly showed that Stx2A accumulated in the R-ER within 1 h after Stx2 addition. We propose that Stx2A in the R-ER may trigger "ER stress" and caspase activation. Others have shown that receptor mediated, internalized Stx or StxB is transported from endosomes via the Golgi apparatus to the ER (48), with migration to the cytosol in HeLa cells (17). In other cell types, brefeldin A blocked the movement of Stx1 into the cytosol and prevented the inhibition of protein synthesis (11) and the apoptosis caused by Stxs (30).

Our data show that Stx1 caused activation of the apoptotic mitochondrial pathway for apoptosis. We conclude that caspase-8 activates Bid protein, a member of the Bcl-2 family of proteins (53) that reacts with and permeabilizes the mitochondrial outer membrane to allow release of cytochrome *c* (7, 9). A complex formed of cytochrome *c* and other factors leads to activation of caspase-9, which is known to indirectly cause DNA fragmentation. However, Stx1 was also found to increase levels of factor XIAP protein, which strongly inhibits caspase-9 activity. The inhibitor of apoptosis (IAP) family is conserved in mammalian cells. XIAP was found to be sufficient for inhibition of apoptosis induced by Fas (52), and the XIAP-ring fragment blocked caspase-9 by directly inhibiting caspase-9 activity (10). This differs from other systems, where cytochrome *c* triggered activation of caspase-9, which then accelerated apoptosis by activating caspase-3. Thus, in the Stx1-HeLa cell model of apoptosis, caspase-8 is a central factor that is required for activation of the mitochondrial pathway and for activation of caspase-3. However, only the caspase-3 pathway appears to be functional in Stx-induced apoptosis of HeLa cells. Whether Stx1 activates caspase-8 and caspase-6 directly or indirectly in the cytosol in HeLa cells is not known.

To understand the upregulation of caspase-8 activity, we tested the concept that Stx1 could be eliciting secretion of TNF-α, which then bound to the HeLa cells and induced apoptosis through well-known receptor-mediated cascades (5). We carried out RT-PCR to examine induction of TNF-α mRNAs in response to Stx1 treatment of HeLa cells. However, neither TNF-α mRNA nor TNF-α protein was detected in Stx1-treated HeLa cells (data not shown). Our results also failed to demonstrate an increase in Fas expression in Stx1-treated HeLa cells. This apoptosis induced by Stx1 in HeLa cells suggests that some new factors might be responsible for activation of caspase-8 in HeLa cells. Kiyokawa et al. also reported that the trigger of caspase-8 activation following Stx1 binding to Burkitt's lymphoma cells was unknown (27). Our data support a new pathway of apoptosis that will require further study for full delineation.

ACKNOWLEDGMENTS

We thank C. Thorpe (Tufts University School of Medicine) for providing Stx2 E166D mutants.

This study was supported by USPHS grants AI24431 and DK52073.

REFERENCES

1. **Adam, S. A., R. S. Marr, and L. Gerace.** 1990. Nuclear protein import in permeabilized mammalian cells requires soluble cytoplasmic factors. J. Cell Biol. **111:**807–816.
2. **Allsopp, T. E., J. McLuckie, L. E. Kerr, M. Macleod, J. Sharkey, and J. S.**

Kelly. 2000. Caspase 6 activity initiates caspase 3 activation in cerebellar granule cell apoptosis. Cell Death Differ. **7:**984–993.
3. **Alnemri, E. S., D. J. Livingston, D. W. Nicholson, G. Salvesen, N. A. Thornberry, W. W. Wong, and J. Yuan.** 1996. Human ICE/CED-3 protease nomenclature. Cell **87:**171.
4. **Arab, S., M. Murakami, P. Dirks, B. Boyd, S. L. Hubbard, C. A. Lingwood, and J. T. Rutka.** 1998. Verotoxins inhibit the growth of and induce apoptosis in human astrocytoma cells. J. Neurooncol. **40:**137–150.
5. **Ashkenazi, A., and V. M. Dixit.** 1998. Death receptors: signaling and modulation. Science **281:**1305–1308.
6. **Bitko, V., and S. Barik.** 1998. Persistent activation of RelA by respiratory syncytial virus involves protein kinase C, underphosphorylated IκBβ, and sequestration of protein phosphatase 2A by the viral phosphoprotein. J. Virol. **72:**5610–5618.
7. **Bossy-Wetzel, E., and D. R. Green.** 1999. Caspases induce cytochrome *c* release from mitochondria by activating cytosolic factors. J. Biol. Chem. **274:**17484–17490.
8. **Burton, K.** 1956. A study of the conditions and mechanism of the diphenylamine reaction for the colorimetric estimation of deoxyribonucleic acid. Biochem. J. **62:**315–323.
9. **Desagher, S., A. Osen-Sand, A. Nichols, R. Eskes, S. Montessuit, S. Lauper, K. Maundrell, B. Antonsson, and J. C. Martinou.** 1999. Bid-induced conformational change of Bax is responsible for mitochondrial cytochrome *c* release during apoptosis. J. Cell Biol. **144:**891–901.
10. **Deveraux, Q. L., E. Leo, H. R. Stennicke, K. Welsh, G. S. Salvesen, and J. C. Reed.** 1999. Cleavage of human inhibitor of apoptosis protein XIAP results in fragments with distinct specificities for caspases. EMBO J. **18:**5242–5251.
11. **Donta, S. T., T. K. Tomicic, and A. Donohue-Rolfe.** 1995. Inhibition of Shiga-like toxins by brefeldin A. J. Infect. Dis. **171:**721–724.
12. **Endo, Y., K. Tsurugi, T. Yutsudo, Y. Takeda, T. Ogasawara, and K. Igarashi.** 1988. Site of action of a Vero toxin (VT2) from *Escherichia coli* O157:H7 and of Shiga toxin on eukaryotic ribosomes. RNA *N*-glycosidase activity of the toxins. Eur. J. Biochem. **171:**45–50.
13. **Falguieres, T., F. Mallard, C. Baron, D. Hanau, C. Lingwood, B. Goud, J. Salamero, and L. Johannes.** 2001. Targeting of Shiga toxin b-subunit to retrograde transport route in association with detergent-resistant membranes. Mol. Biol. Cell **12:**2453–2468.
14. **Finucane, D. M., E. Bossy-Wetzel, N. J. Waterhouse, T. G. Cotter, and D. R. Green.** 1999. Bax-induced caspase activation and apoptosis via cytochrome *c* release from mitochondria is inhibitable by Bcl-xL. J. Biol. Chem. **274:**2225–2233.
15. **Green, D. R., and J. C. Reed.** 1998. Mitochondria and apoptosis. Science **281:**1309–1312.
16. **Hamano, S., Y. Nakanishi, T. Nara, T. Seki, T. Ohtani, T. Oishi, K. Joh, T. Oikawa, Y. Muramatsu, Y. Ogawa, et al.** 1993. Neurological manifestations of hemorrhagic colitis in the outbreak of *Escherichia coli* O157:H7 infection in Japan. Acta Paediatr. **82:**454–458.
17. **Hazes, B., and R. J. Read.** 1997. Accumulating evidence suggests that several AB-toxins subvert the endoplasmic reticulum-associated protein degradation pathway to enter target cells. Biochemistry **36:**11051–11054.
18. **Heibein, J. A., M. Barry, B. Motyka, and R. C. Bleackley.** 1999. Granzyme B-induced loss of mitochondrial inner membrane potential ($\Delta\Psi_m$) and cytochrome *c* release are caspase independent. J. Immunol. **163:**4683–4693.
19. **Inward, C. D., J. Williams, I. Chant, J. Crocker, D. V. Milford, P. E. Rose, and C. M. Taylor.** 1995. Verocytotoxin-1 induces apoptosis in Vero cells. J. Infect. **30:**213–218.
20. **Jones, N. L., A. Islur, R. Haq, M. Mascarenhas, M. A. Karmali, M. H. Perdue, B. W. Zanke, and P. M. Sherman.** 2000. *Escherichia coli* Shiga toxins induce apoptosis in epithelial cells that is regulated by the Bcl-2 family. Am. J. Physiol. Gastrointest. Liver Physiol. **278:**G811–G819.
21. **Kaneko, K., N. Kiyokawa, Y. Ohtomo, R. Nagaoka, Y. Yamashiro, T. Taguchi, T. Mori, J. Fujimoto, and T. Takeda.** 2001. Apoptosis of renal tubular cells in Shiga-toxin-mediated hemolytic uremic syndrome. Nephron **87:**182–185.
22. **Karmali, M. A.** 1989. Infection by verocytotoxin-producing *Escherichia coli*. Clin. Microbiol. Rev. **2:**15–38.
23. **Karmali, M. A., M. Petric, C. Lim, P. C. Fleming, G. S. Arbus, and H. Lior.** 1985. The association between idiopathic hemolytic uremic syndrome and infection by verotoxin-producing *Escherichia coli*. J. Infect. Dis. **151:**775–782.
24. **Karmali, M. A., B. T. Steele, M. Petric, and C. Lim.** 1983. Sporadic cases of haemolytic-uraemic syndrome associated with faecal cytotoxin and cytotoxin-producing *Escherichia coli* in stools. Lancet **i:**619–620.
25. **Karpman, D., A. Hakansson, M. T. Perez, C. Isaksson, E. Carlemalm, A. Caprioli, and C. Svanborg.** 1998. Apoptosis of renal cortical cells in the hemolytic-uremic syndrome: in vivo and in vitro studies. Infect. Immun. **66:**636–644.
26. **Kita, E., Y. Yunou, T. Kurioka, H. Harada, S. Yoshikawa, K. Mikasa, and N. Higashi.** 2000. Pathogenic mechanism of mouse brain damage caused by oral infection with Shiga toxin-producing *Escherichia coli* O157:H7. Infect. Immun. **68:**1207–1214.
27. **Kiyokawa, N., T. Mori, T. Taguchi, M. Saito, K. Mimori, T. Suzuki, T. Sekino, N. Sato, H. Nakajima, Y. U. Katagiri, T. Takeda, and J. Fujimoto.** 2001. Activation of the caspase cascade during Stx1-induced apoptosis in Burkitt's lymphoma cells. J. Cell. Biochem. **81:**128–142.
28. **Kiyokawa, N., T. Taguchi, T. Mori, H. Uchida, N. Sato, T. Takeda, and J. Fujimoto.** 1998. Induction of apoptosis in normal human renal tubular epithelial cells by *Escherichia coli* Shiga toxins 1 and 2. J. Infect. Dis. **178:**178–184.
29. **Kodama, T., K. Nagayama, K. Yamada, Y. Ohba, Y. Akeda, and T. Honda.** 1999. Induction of apoptosis in human renal proximal tubular epithelial cells by *Escherichia coli* verocytotoxin 1 in vitro. Med. Microbiol. Immunol.(Berlin) **188:**73–78.
30. **Kojio, S., H. Zhang, M. Ohmura, F. Gondaira, N. Kobayashi, and T. Yamamoto.** 2000. Caspase-3 activation and apoptosis induction coupled with the retrograde transport of Shiga toxin: inhibition by brefeldin A. FEMS Immunol. Med. Microbiol. **29:**275–281.
31. **Li, P., D. Nijhawan, I. Budihardjo, S. M. Srinivasula, M. Ahmad, E. S. Alnemri, and X. Wang.** 1997. Cytochrome *c* and dATP-dependent formation of Apaf-1/caspase-9 complex initiates an apoptotic protease cascade. Cell **91:**479–489.
32. **Lingwood, C. A.** 1996. Role of verotoxin receptors in pathogenesis. Trends Microbiol. **4:**147–153.
33. **Lingwood, C. A., H. Law, S. Richardson, M. Petric, J. L. Brunton, S. De Grandis, and M. Karmali.** 1987. Glycolipid binding of purified and recombinant *Escherichia coli* produced verotoxin in vitro. J. Biol. Chem. **262:**8834–8839.
34. **Liu, X., C. N. Kim, J. Yang, R. Jemmerson, and X. Wang.** 1996. Induction of apoptotic program in cell-free extracts: requirement for dATP and cytochrome *c*. Cell **86:**147–157.
35. **Mallard, F., C. Antony, D. Tenza, J. Salamero, B. Goud, and L. Johannes.** 1998. Direct pathway from early/recycling endosomes to the Golgi apparatus revealed through the study of Shiga toxin B-fragment transport. J. Cell Biol. **143:**973–990.
36. **Mangeney, M., C. A. Lingwood, S. Taga, B. Caillou, T. Tursz, and J. Wiels.** 1993. Apoptosis induced in Burkitt's lymphoma cells via Gb3/CD77, a glycolipid antigen. Cancer Res. **53:**5314–5319.
37. **Mayhew, T. M., J. M. Lucocq, and G. Griffiths.** 2002. Relative labelling index: a novel stereological approach to test for non-random immunogold labelling of organelles and membranes on transmission electron microscopy thin sections. J. Microsc. **205:**153–164.
38. **Michino, H., K. Araki, S. Minami, S. Takaya, N. Sakai, M. Miyazaki, A. Ono, and H. Yanagawa.** 1999. Massive outbreak of *Escherichia coli* O157:H7 infection in schoolchildren in Sakai City, Japan, associated with consumption of white radish sprouts. Am. J. Epidemiol. **150:**787–796.
39. **Morris, R. E., and G. M. Ciraolo.** 1997. A universal post-embedding protocol for immunogold labelling of osmium-fixed, epoxy resin-embedded tissue. J. Electron Microsc. (Tokyo) **46:**315–319.
40. **Morris, R. E., G. M. Ciraolo, and C. B. Saelinger.** 1992. Validation of the biotinyl ligand-avidin-gold technique. J. Histochem. Cytochem. **40:**711–721.
41. **Nakagawa, I., M. Nakata, S. Kawabata, and S. Hamada.** 1999. Regulated expression of the Shiga toxin B gene induces apoptosis in mammalian fibroblastic cells. Mol. Microbiol. **33:**1190–1199.
42. **Nudelman, E., R. Kannagi, S. Hakomori, M. Parsons, M. Lipinski, J. Wiels, M. Fellous, and T. Tursz.** 1983. A glycolipid antigen associated with Burkitt lymphoma defined by a monoclonal antibody. Science **220:**509–511.
43. **O'Brien, A. D., and R. K. Holmes.** 1987. Shiga and Shiga-like toxins. Microbiol. Rev. **51:**206–220.
44. **Obrig, T. G., T. P. Moran, and J. E. Brown.** 1987. The mode of action of Shiga toxin on peptide elongation of eukaryotic protein synthesis. Biochem. J. **244:**287–294.
45. **Orci, L., M. Tagaya, M. Amherdt, A. Perrelet, J. G. Donaldson, J. Lippincott-Schwartz, R. D. Klausner, and J. E. Rothman.** 1991. Brefeldin A, a drug that blocks secretion, prevents the assembly of non-clathrin-coated buds on Golgi cisternae. Cell **64:**1183–1195.
46. **Riley, L. W., R. S. Remis, S. D. Helgerson, H. B. McGee, J. G. Wells, B. R. Davis, R. J. Hebert, E. S. Olcott, L. M. Johnson, N. T. Hargrett, P. A. Blake, and M. L. Cohen.** 1983. Hemorrhagic colitis associated with a rare *Escherichia coli* serotype. N. Engl. J. Med. **308:**681–685.
47. **Ruchaud, S., N. Korfali, P. Villa, T. J. Kottke, C. Dingwall, S. H. Kaufmann, and W. C. Earnshaw.** 2002. Caspase-6 gene disruption reveals a requirement for lamin A cleavage in apoptotic chromatin condensation. EMBO J. **21:**1967–1977.
48. **Sandvig, K., M. Ryd, O. Garred, E. Schweda, P. K. Holm, and B. van Deurs.** 1994. Retrograde transport from the Golgi complex to the ER of both Shiga toxin and the nontoxic Shiga B-fragment is regulated by butyric acid and cAMP. J. Cell Biol. **126:**53–64.
49. **Sandvig, K., and B. van Deurs.** 1996. Endocytosis, intracellular transport, and cytotoxic action of Shiga toxin and ricin. Physiol. Rev. **76:**949–966.
50. **Taga, S., K. Carlier, Z. Mishal, C. Capoulade, M. Mangeney, Y. Lecluse, D. Coulaud, C. Tetaud, L. L. Pritchard, T. Tursz, and J. Wiels.** 1997. Intracellular signaling events in CD77-mediated apoptosis of Burkitt's lymphoma cells. Blood **90:**2757–2767.
51. **Takahashi, A., E. S. Alnemri, Y. A. Lazebnik, T. Fernandes-Alnemri, G. Litwack, R. D. Moir, R. D. Goldman, G. G. Poirier, S. H. Kaufmann, and W. C. Earnshaw.** 1996. Cleavage of lamin A by Mch2α but not CPP32:

multiple interleukin 1β-converting enzyme-related proteases with distinct substrate recognition properties are active in apoptosis. Proc. Natl. Acad. Sci. USA **93:**8395–8400.
52. **Takahashi, R., Q. Deveraux, I. Tamm, K. Welsh, N. Assa-Munt, G. S. Salvesen, and J. C. Reed.** 1998. A single BIR domain of XIAP sufficient for inhibiting caspases. J. Biol. Chem. **273:**7787–7790.
53. **Tang, D., J. M. Lahti, and V. J. Kidd.** 2000. Caspase-8 activation and Bid cleavage contribute to MCF7 cellular execution in a caspase-3-dependent manner during staurosporine-mediated apoptosis. J. Biol. Chem. **275:**9303–9307.
54. **Tesh, V. L., and A. D. O'Brien.** 1991. The pathogenic mechanisms of Shiga toxin and the Shiga-like toxins. Mol. Microbiol. **5:**1817–1822.
55. **Uchida, H., N. Kiyokawa, T. Taguchi, H. Horie, J. Fujimoto, and T. Takeda.** 1999. Shiga toxins induce apoptosis in pulmonary epithelium-derived cells. J. Infect. Dis. **180:**1902–1911.
56. **Wiels, J.** 2000. CD77. J. Biol. Regul. Homeost. Agents **14:**288–289.
57. **Yang, J., X. Liu, K. Bhalla, C. N. Kim, A. M. Ibrado, J. Cai, T. I. Peng, D. P. Jones, and X. Wang.** 1997. Prevention of apoptosis by Bcl-2: release of cytochrome *c* from mitochondria blocked. Science **275:**1129–1132.
58. **Yasuhara, A., A. Araki, A. Ochi, and Y. Kobayashi.** 2000. Magnetic resonance imaging of brain lesions of a patient with hemolytic uremic syndrome following *Escherichia coli* O157 infection. Pediatr. Int. **42:**302–305.
59. **Yutsudo, T., N. Nakabayashi, T. Hirayama, and Y. Takeda.** 1987. Purification and some properties of a Vero toxin from *Escherichia coli* O157:H7 that is immunologically unrelated to Shiga toxin. Microb. Pathog. **3:**21–30.

Editor: A. D. O'Brien